Eur. Phys. J. A **8**, 283–289 (2000)

THE EUROPEAN PHYSICAL JOURNAL A

Pion scalar density and chiral symmetry restoration at finite temperature and density

G. Chanfray[1,a], D. Davesne[1], J. Delorme[1], M. Ericson[1,2], and J. Marteau[1]

[1] Institute de Physique Nucléaire de Lyon, IN2P3-CNRS et Université Cl. Bernard, 43, Bvd. du 11 novembre 1918, F-69622 Villeurbanne Cedex, France
[2] CERN, Theory Division, CH-1211 Geneva 23, Switzerland

Received: 7 December 1999 / Revised version: 31 March 2000
Communicated by W. Weise

Abstract. This paper is devoted to the evaluation of the pionic scalar density at finite temperature and baryonic density. We express the latter effect in terms of the nuclear response evaluated in the random phase approximation. We discuss the density and temperature evolution of the pionic density which governs the quark condensate evolution. Numerical evaluations are performed.

PACS. 14.40.Aq π, K and η mesons – 24.85.+p Quarks, gluons, and QCD in nuclei and nuclear processes

1 Introduction

Pions play a crucial role in chiral symmetry restoration, due to their Goldstone boson character. The amount of restoration is measured by the modification of the order parameter, *i.e.* the quark condensate density, with respect to the vacuum value. In this context the evaluation of the expectation value of the squared pion field, linked to the scalar density of pions $\rho_{\rm S}^{\pi}$ by $\rho_{\rm S}^{\pi} = m_\pi \langle \Phi^2 \rangle$, is of a great interest. For a single nucleon this quantity governs the total amount of chiral symmetry restoration of pionic origin, according to [1,2]:

$$\frac{m_\pi^2}{2} \int {\rm d}^3\mathbf{x} \langle N|\Phi^2(x)|N\rangle = 2m_q \int {\rm d}^3\mathbf{x} \langle N|\Delta^\pi \overline{q}q(x)|N\rangle = \Sigma_N^\pi = \frac{m_\pi}{2} N_\pi, \qquad (1)$$

where N_π is the scalar number of pions in the nucleon cloud, Σ_N^π is the part of the nucleon Σ commutator of pionic origin and $\langle N|\Delta^\pi \overline{q}q(x)|N\rangle$ represents the corresponding modification of the quark condensate with respect to the vacuum value. Similarly, in a uniform nuclear medium of density ρ, or in a heat bath, the evolution of the quark condensate originating from the pions is linked, to one-pion loop order, to the average value $\langle \Phi^2 \rangle$ by

$$\frac{\Delta^\pi \langle \bar{q}q(\rho,T)\rangle}{\langle \bar{q}q(0,0)\rangle} = -\frac{\langle \Phi^2 \rangle}{2f_\pi^2}. \qquad (2)$$

The same quantity $\langle \Phi^2 \rangle$ governs also the quenching factor, $1 - \langle \Phi^2 \rangle / 3f_\pi^2$, of coupling constants such as the nucleonic axial coupling constant $g_{\rm A}$ or the pion decay one f_π, originating from pion loops, which is the counterpart of the mixing of axial and vector currents [3,4]. This type of quenching has to be seen as a manifestation of chiral symmetry restoration and should also apply to the case of ρ-meson excitation by virtual photons as enters in relativistic heavy-ion collisions. It is therefore interesting to evaluate the quantity $\langle \Phi^2 \rangle$ in the conditions of such experiments. Now, the fireball which is the source of the dileptons contains, besides thermal pions, a significant residual baryonic background We have therefore to understand how the pion density evolves at finite values of both temperature and baryonic chemical potential. The first-order approximation for the quantity $\langle \Phi^2 \rangle$ adds the values for a pure heat bath and for a cold baryonic medium, writing with obvious notations:

$$\langle \Phi^2 \rangle(\rho,T) = \langle \Phi^2 \rangle_T(\rho=0) + \langle \Phi^2 \rangle_\rho(T=0). \qquad (3)$$

However, this approximation is likely to be crude since the temperature has an effect on the pion density of the nuclear medium and on the other hand the presence of the baryonic background modifies the number of pions thermally excited. As an illustration of the second point, the pion density in the baryonic vacuum is fixed by the Bose-Einstein factor which is $(e^{\omega_k/T} - 1)^{-1}$ for pions of momentum $\mathbf{k}$, with $\omega_k = \sqrt{\mathbf{k}^2 + m_\pi^2}$. In the nuclear medium the pion becomes a quasi-particle with a broad width. It can decay for instance into a particle-hole pair which has a smaller energy than the free pion. Its excitation is then favored by the thermal factor. There is therefore a mutual influence between temperature and density that we will investigate.

[a] e-mail: g.chanfray@ipnl.in2p3.fr

$$N_\pi = m_\pi \int \mathrm{d}^3\mathbf{x}\langle N|\Phi^2(\mathbf{x}|N\rangle = m_\pi\, 3\,\frac{g^2_{\pi NN}}{4M^2}$$
$$\times \int \frac{\mathrm{d}^3q}{(2\pi)^3}\boldsymbol{q}^2\Bigg\{\frac{1}{\omega_q}\left[\frac{1}{2\omega_q}\frac{1}{(\varepsilon_q+\omega_q)^2}+\frac{1}{2\omega_q^2}\frac{1}{(\varepsilon_q+\omega_q)}\right]v^2(Q^2)+\frac{4}{9}\left(\frac{g_{\pi N\Delta}}{g_{\pi NN}}\right)^2$$
$$\times\int_0^\infty\frac{\mathrm{d}\omega}{\omega_q}\left[\frac{1}{2\omega_q}\frac{1}{(\omega+\omega_q)^2}+\frac{1}{2\omega_q^2}\frac{1}{(\omega+\omega_q)}\right]v^2(Q^2)\left(-\frac{1}{\pi}\,\mathrm{Im}\,\frac{1}{\omega-\omega_\Delta+i(\Gamma_\Delta/2)}\right)\Bigg\}. \quad (9)$$

The article is organized as follows. In the second section we evaluate the pion density of a nuclear medium at zero temperature. We relate this quantity to the nuclear response to a pion-like excitation. We evaluate this response in the RPA scheme, taking also into account the two particle-two hole(2p-2h) excitations. Within this framework, we study the deviation with respect to the independent nucleon approximation. In the third section we introduce the effect of the temperature through the modification of the nuclear responses. In the fourth section we incorporate the influence of the finite baryonic chemical potential in the heat bath case.

2 Pion scalar density in the cold nuclear medium

This quantity was discussed in relation to the quark condensate modification by Chanfray and Ericson [1]. They discussed its deviations with respect to free nucleons, introducing the nuclear response to pion-like excitation, treated in the static case $M_N \to \infty$. The extension to the non-static situation can be performed through the time-ordered graphs of fig. 1 where the cross represents the point at which the pions are created or annihilated. The pion momentum is denoted q and ω is the excitation energy of the nuclear system in the intermediate state. The sum of the four graphs leads to the following expression which has also been derived with a different method in ref. [5]:

$$\langle\Phi^2\rangle = \frac{\rho}{A}\,3\,\frac{g^2_{\pi\mathrm{NN}}}{4M^2_\mathrm{N}}\int\frac{\mathrm{d}^3q}{(2\pi)^3\,2\omega_q^2}$$
$$\times\int_0^\infty\mathrm{d}\omega\left[\frac{1}{(\omega+\omega_q)^2}+\frac{1}{\omega_q}\frac{1}{(\omega+\omega_q)}\right]$$
$$\times v^2\big(Q^2\big)R_\mathrm{L}(\omega,\boldsymbol{q}), \quad (4)$$

where $Q^2=\omega^2-\boldsymbol{q}^2$, $v(Q^2)$ is the form factor of the pion vertex for which we use a monopole form

$$v\big(Q^2\big)=\frac{\Lambda^2-m_\pi^2}{\Lambda^2-Q^2}. \quad (5)$$

Finally, R_L represents the spin-isospin longitudinal response function:

$$R_\mathrm{L}(\omega,\boldsymbol{q})=\sum_n\left|\left\langle n\left|\sum_{i=1}^A\sigma_i\cdot\boldsymbol{q}\tau_i^a e^{i\boldsymbol{q}\cdot\boldsymbol{r}_i}\right|0\right\rangle\right|^2\delta(\omega-E_n). \quad (6)$$

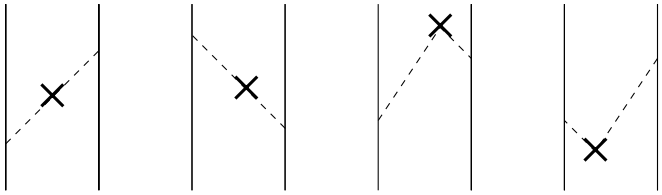

Fig. 1. Time-ordered graphs for pion exchange.

In the actual calculation, we add in the response R_L the excitation of the delta-resonance with the standard replacement:

$$\boldsymbol{\sigma}_i\cdot\boldsymbol{q}\tau_i^a\longrightarrow\frac{g_{\pi\mathrm{N}\Delta}}{g_{\pi\mathrm{NN}}}\boldsymbol{S}_i^\dagger\cdot\boldsymbol{q}(T_i^a)^\dagger, \quad (7)$$

where $\boldsymbol{S}^\dagger(\boldsymbol{T}^\dagger)$ is the spin (isospin) transition operator connecting the spin (isospin) $\frac{1}{2}$ and $\frac{3}{2}$ states [6]. Note that for a matter of convenience we have incorporated in this operator the ratio of the $\pi\mathrm{N}\Delta$ and $\pi\mathrm{NN}$ coupling constants. We have also assumed the same form factors, $v(Q^2)$, at the $\pi\mathrm{NN}$ vertex and at the $\pi\mathrm{N}\Delta$ vertices. Finally we recall the link between the response function and the polarization propagator $\Pi(\omega,\boldsymbol{q},\boldsymbol{q'})$ which we will use in the following:

$$R(\omega,\boldsymbol{q})=-\frac{V}{\pi}\,\mathrm{Im}\,\Pi(\omega,\boldsymbol{q},\boldsymbol{q}). \quad (8)$$

We will first discuss the result for the free nucleon.

2.1 Free nucleon

In the nucleon case, where the response R_L reduces to a simple expression, eq. (4) provides for the (scalar) pion number N_π in the nucleon cloud:

see equation (9) *above*

In the above equation we have used the following notations: $\varepsilon_q=\boldsymbol{q}^2/2M_\mathrm{N}$ and $\omega_\Delta=M_\Delta-M_\mathrm{N}+\boldsymbol{q}^2/2M_\Delta$. The energy dependence of the delta width Γ_Δ is taken from the analysis of the pion-nucleon scattering [6].

Our numerical inputs for the evaluation of N_π are defined as follows. Without form-factor the integrals diverge linearly. The resulting value is then quite sensitive to the cut-off function. We stress, however, that the specific case of the single nucleon is not the purpose of this paper.

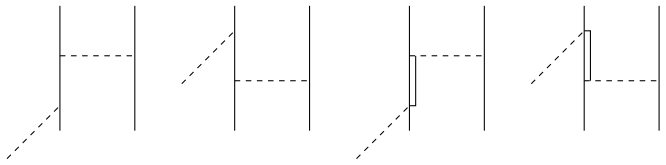

Fig. 2. Feynman diagrams for the 2p-2h processes. The double line represents the delta-resonance.

It is for us an element of comparison to introduce the nuclear effects. Since we want to restrict the calculation to a region where nuclear effects are reasonably under control, we have limited the integrals to: $q = 1\,\mathrm{GeV}$ and $\omega = 1\,\mathrm{GeV}$. The parameters are chosen so as to obtain a value $\Sigma_N^\pi = \frac{1}{2} m_\pi N_\pi = 30\,\mathrm{MeV}$ which is well in the accepted range [7–9]. This is achieved with $\Lambda = 1\,\mathrm{GeV}$ and $(g_{\pi \mathrm{N}\Delta}/g_{\pi \mathrm{NN}})^2 = 3.8$.

2.2 Infinite nuclear matter

We now turn to the case of infinite nuclear matter. In order to evaluate the response functions, we use the method of Delorme and Guichon [10] who calculated the zeroth-order response in the local density approximation and then solved exactly the RPA equations. Their zeroth-order response function also includes the 2p-2h excitations. The corresponding Feynman diagrams of such processes are displayed in fig. 2.

They are calculated in two steps. First we single out the contributions which reduce to a medium modification of the Δ self-energy, for which the parametrization of ref. [11] is used. This parametrization includes some 3p-3h excitation states as well. For the rest we use the results of Shimizu-Faessler [12] who evaluated the two nucleons p-wave pion absorption at threshold ($\omega = m_\pi$), from which the Δ self-energy part, already taken into account, is separated out. As for each the remaining contributions, an energy extrapolation suggested by the many-body diagrammatic interpretation is performed.

We solve the RPA equations in the ring approximation: $\Pi = \Pi^0 + \Pi^0 \mathcal{V} \Pi$. Here $\mathcal{V}$ is the particle-hole (p-h) interaction with the standard formulation: $\mathcal{V} = V_\pi + V_{g'}$, where the second piece is the short-range Landau-Migdal part. More explicitly with our definition of the response, $\mathcal{V}$ reads

$$\mathcal{V} = \frac{v^2(Q^2)}{\boldsymbol{q}^2} \left(\frac{\boldsymbol{q}^2}{Q^2 - m_\pi^2} + g' \right). \tag{10}$$

The corresponding Landau-Migdal parameters g' are different in the various channels: g'_{NN} for the NN sector, $g'_{\Delta\Delta}$ for the Δ one, $g'_{\mathrm{N}\Delta}$ for the mixing of NN and ΔN excitations. We adopt the following values:

$$g'_{\mathrm{NN}} = 0.7, \qquad g'_{\mathrm{N}\Delta} = g'_{\Delta\Delta} = 0.5. \tag{11}$$

The results are illustrated on fig. 3 which shows the energy dependence of the zeroth-order and RPA responses, for a fixed value of the momentum $q = 300\,\mathrm{MeV}$. The

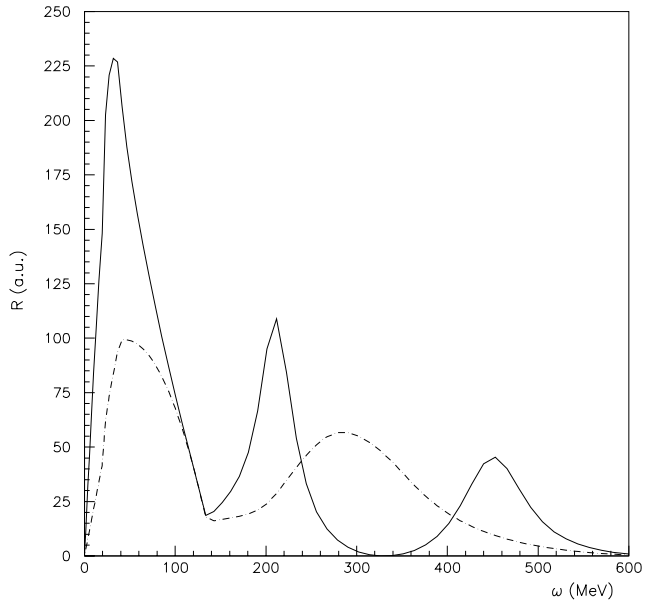

Fig. 3. Response function per nucleon at normal nuclear density as a function of the energy for a fixed momentum $q = 300\,\mathrm{MeV}$. The dot-dashed and continuous lines represent, respectively, the zeroth-order and RPA responses.

bare response presents a low-energy peak corresponding to the NN^{-1} excitation and a high-energy one ($\Delta\mathrm{N}^{-1}$ excitations). The figure displays the RPA enhancement of the low-energy peak, introduced by Alberico *et al.* [13], which arises from the attractive nature of the p-h interaction. It also displays the collective behaviour of the Δ excitation with a splitting into two branches.

Once the energy and momentum integrations are performed, we find, as in ref. [1], a moderate increase as compared to the free nucleon value, with the values per nucleon at normal nuclear density:

$$\tilde{\Sigma}_N^\pi \equiv \frac{\Sigma_A^\pi}{A} = 38.5\,\mathrm{MeV} \qquad \text{and} \qquad \frac{N_A^\pi}{A} = 0.55 \tag{12}$$

versus 30 MeV and 0.40, respectively, for the free nucleon. The quantity $\tilde{\Sigma}_{\mathrm{N}}^\pi$ is the (medium modified) effective sigma commutator.

More precisely, we decompose the response function Π (accordingly Σ^π) into four types, depending on the kind of states which are excited at each external vertices: NN, NΔ, ΔN and $\Delta\Delta$ (fig. 4). The density evolution of the different components of the sigma commutator are represented in fig. 5 both without and with RPA. Notice that, in the absence of the RPA, there is already a contribution of the NΔ channel at finite density due to the 2p-2h excitations. The overall RPA increase of the sigma commutator mainly comes from that of the $\Sigma_{\mathrm{N}\Delta} + \Sigma_{\Delta\mathrm{N}}$ parts. These last quantities embody the mixing of the $\Delta\mathrm{N}^{-1}$ configurations into the NN^{-1} ones. This is well known to be responsible for the enhancement Ä of the low-energy response (*i.e.* the NN^{-1} excitations) [14].

$$L_{ab^{-1}}(\omega,\mathbf{q}) = -\frac{N_{\mathrm{S,I}}}{4\pi^2}\int k^2\,\mathrm{d}k\,\mathrm{d}(\cos\theta)\frac{f(\omega_k^b)(1-f(\omega_{k+q}^a))}{\omega-\omega_{k+q}^a+\omega_k^b+\frac{i}{2}\Gamma^a(\omega_k^b+\omega)+\frac{i}{2}\Gamma^b(\omega_{k+q}^a-\omega)} - \frac{f(\omega_k^b)(1-f(\omega_{k+q}^a))}{\omega+\omega_{k+q}^a-\omega_k^b+\frac{i}{2}\Gamma^a(\omega_k^b-\omega)+\frac{i}{2}\Gamma^b(\omega_{k+q}^a+\omega)}, \tag{13}$$

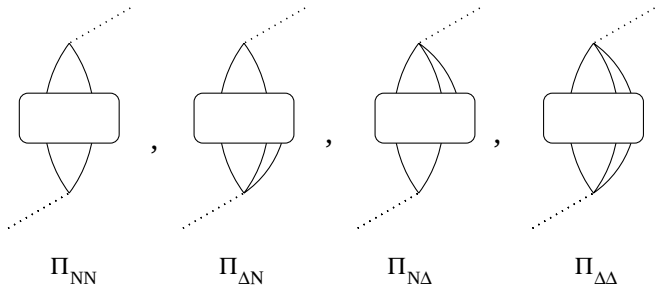

Fig. 4. Symbolic representation of the NN, ΔN, NΔ and $\Delta\Delta$ response functions. The delta-resonance is represented by the double line.

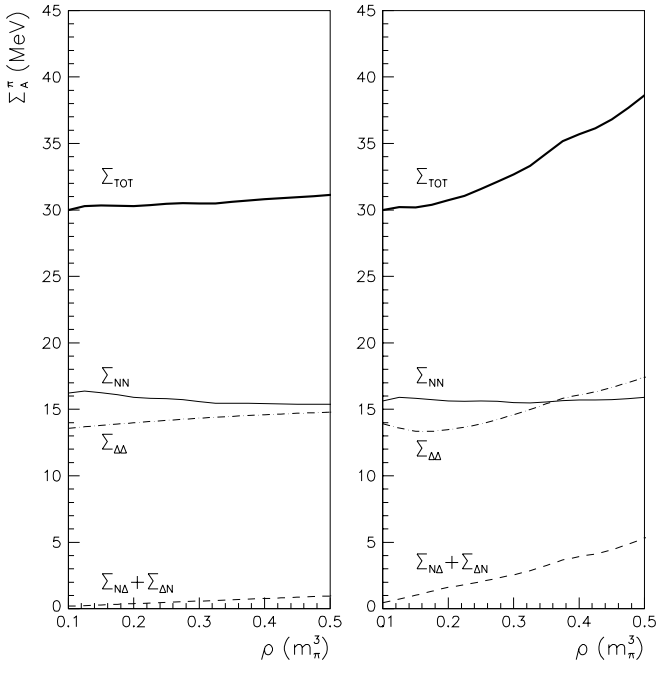

Fig. 5. Density evolution of the different components of the effective sigma commutator: left (right) figure is without (with) RPA.

3 Inclusion of temperature

3.1 Influence on the virtual pion cloud

We now introduce the temperature, *via* the Matsubara formalism: all the integrals over energy are replaced by an infinite sum over Matsubara frequencies. For the NN^{-1} sector, the generalized Lindhart function (the imaginary part of which is proportional to the response function) at finite temperature is discussed in textbooks (see, *e.g.*, ref. [15]). The result is the replacement of the Heaviside functions that characterize the occupation of fermion states at zero temperature by the Fermi-Dirac distributions. We have generalized this procedure to particle with width and applied it to Δ-N^{-1}, N-Δ^{-1} and Δ-Δ^{-1} rings. The generalized Lindhart function $L_{ab^{-1}}$ for a process involving a particle of type (a) and a hole of type (b) is found to be

see equation (13) *above*

where $N_{\mathrm{S,I}}$ is a constant arising from the summation of spin and isospin and $\Gamma^{a,b}(\omega)$ represents the width of the particle of type (a,b) for an energy ω. The occupation number of hadron species a is

$$f(\omega_k^a) = \frac{1}{\exp((\omega_k^a-\mu)/T)+1}, \tag{14}$$

where μ is the (common) chemical potential for baryons, the value of which fixes the baryonic density ρ at a given temperature. As implicitly stated before, we limit ourselves to nucleons and deltas, *i.e.* $\rho = \rho_{\mathrm{N}} + \rho_\Delta$.

Concerning the Δ width, things are somewhat more complicated. In the medium, the pionic decay channel $\Delta \to \pi\mathrm{N}$ is partly suppressed due to Pauli blocking. At the same time, other channels open, the pion being replaced by 1p-1h, 2p-2h, etc. At normal density and zero temperature the pionic channel remains dominant according to ref. [11]. It represents approximatively 75% of the total width ($\simeq$ 90 MeV to be compared with 120 MeV at the resonance energy) and the non-pionic decay channels only the remaining 25%. In view of the difficulties of a full calculation of the temperature effects, we have adopted the simplified following strategy: we have kept the parametrization of ref. [11], derived at $T = 0$, for the non-pionic decay channel. We have introduced the temperature effects *via* the Matsubara formalism only for the main pionic part of the width.

Figure 6 displays the temperature evolutiom of the zeroth-order response function. The dashed line, which represents the $T = 0$ case, exhibits the NN^{-1} and $\Delta\mathrm{N}^{-1}$ structures. Increasing temperature tends to wash out more and more these peaks. At the same time an overall suppression effect occurs. Note that the Δ branch is less affected by the temperature because of the higher energies involved. In the RPA case (see fig. 7), one observes a similar behavior: an important general decrease and the loss of the lower energy structures.

We now turn to the question of the thermal pions present in the heat bath.

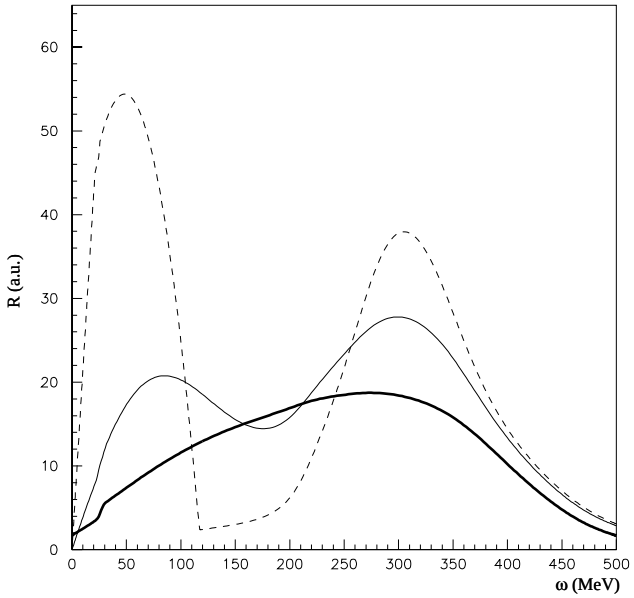

Fig. 6. Zeroth-order response at a baryonic density equal to half nuclear matter density ($\rho = 0.25\,\mathrm{m}_\pi^3$) as a function of energy for a fixed momentum $q = 300\,\mathrm{MeV}$ for three temperatures. Dashed lines: $T = 0$. Thin full line: $T = 50\,\mathrm{MeV}$. Thick full line: $T = 150\,\mathrm{MeV}$.

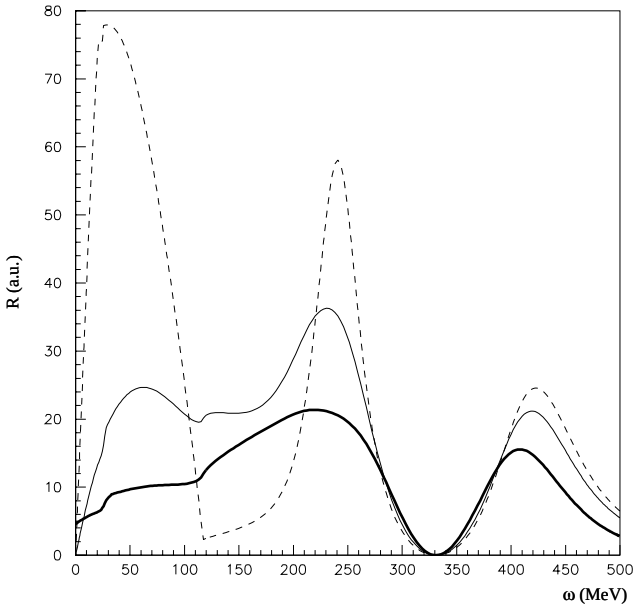

Fig. 7. Same as before but for the RPA response.

3.2 Inclusion of thermal pions

The effects previously discussed concerned only the modification, due to the temperature, of the virtual pion density present in the nuclear medium. At finite temperature, thermally excited pionic modes (quasi-pions) are also present and they give an additional contribution to the pion scalar density. Here for a better illustration we give the result for $\langle \Phi^2 \rangle / 2f_\pi^2$ which according to eq. (2) governs the amount of chiral symmetry restoration of pionic origin. We start from the general result given in ref. [5]:

$$\frac{\langle \Phi^2 \rangle}{2f_\pi^2} = \frac{3}{2f_\pi^2} \int \frac{\mathrm{d}^3 q}{(2\pi)^3} \times \int_0^\infty \mathrm{d}\omega \Big[(1 + 2n(\omega)) \Big(-\frac{1}{\pi} \Big) \,\mathrm{Im}\, D(\omega, \boldsymbol{q}) - \Big(-\frac{1}{\pi} \Big) \,\mathrm{Im}\, D_0(\omega, \boldsymbol{q}) \Big],$$

where the vacuum contribution has been explicitly subtracted. In the above equation $n(\omega) = 1/(\exp(\omega/T) - 1)$ is the Bose occupation factor and $D^{-1}(\omega, \boldsymbol{q}) = D_0^{-1}(\omega, \boldsymbol{q}) - (g_{\pi \mathrm{NN}}/2M_\mathrm{N})^2 k^2 \Pi$ the inverse quasi-pion propagator. For convenience, we separate the contribution surviving at zero temperature expressible in terms of the full spin-isospin longitudinal response function from the contribution with an explicit thermal factor:

$$\begin{aligned} \frac{\langle \Phi^2 \rangle}{2f_\pi^2} &= \frac{\rho}{A} \frac{3}{2f_\pi^2} \frac{g_{\pi \mathrm{NN}}^2}{4M_\mathrm{N}^2} \int \frac{\mathrm{d}^3 q}{(2\pi)^3} \times \int_0^\infty \mathrm{d}\omega \Big(\frac{1}{2\omega_q^2 (\omega + \omega_q)^2} + \frac{1}{2\omega_q^3 (\omega + \omega_q)} \Big) \\ &\quad \times v^2(Q^2) R_L(\omega, \boldsymbol{q}) + \frac{3}{2f_\pi^2} \int \frac{\mathrm{d}^3 q}{(2\pi)^3} \\ &\quad \times \int_0^\infty \mathrm{d}\omega \, n(\omega) \Big(-\frac{2}{\pi} \Big) \,\mathrm{Im}\, D(\omega, \boldsymbol{q}) \\ &\equiv \frac{\rho \tilde{\Sigma}_B^\pi}{f_\pi^2 m_\pi^2} + \frac{\langle \Phi^2 \rangle_T}{2f_\pi^2}. \end{aligned}$$

The second identity defines the quantities $\tilde{\Sigma}_B^\pi$ and $\langle \Phi^2 \rangle_T$, associated, respectively, with the first and second pieces of the r.h.s. of the above equation: $\tilde{\Sigma}_B^\pi$ represents an effective, temperature-dependent, sigma commutator per baryon, whereas $\langle \Phi^2 \rangle_T$ is the scalar density of quasi-pions thermally excited.

4 Results

In order to display the condensate evolution, all the forthcoming figures show its relative decrease, *i.e.* the quantity $\Phi^2/2f_\pi^2$ according to eq. (2). We stress again that the points of interest are the influence of temperature on the nuclear pionic cloud contribution, the influence of the baryonic density on the thermal pions one and finally how large is the deviation from the additive approximation of eq. (3).

We first present on fig. 8 the contribution of the virtual pion cloud alone (term in $\tilde{\Sigma}_B^\pi$). Each box shows the temperature evolution at fixed baryonic density. It illustrates the suppression effect of the temperature which originates in the quenching of the nuclear response previously mentioned. The increase with baryonic density observed in this figure reflects the obvious fact that the pionic density follows the baryon one.

In fig. 9 we present in the same fashion the condensate decrease due to thermal pions alone (term in $\langle \Phi^2 \rangle_T / 2f_\pi^2$).

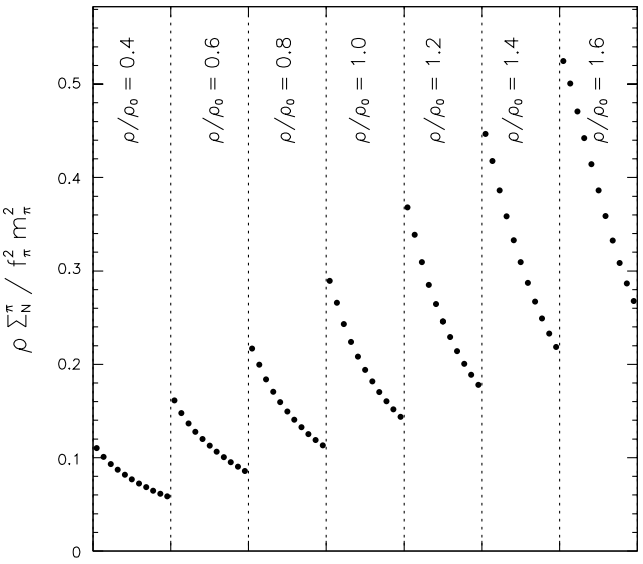

Fig. 8. Relative decrease of the condensate coming from the virtual pion cloud part as a function of the density and the temperature. Each box corresponds to a fixed density as indicated. The density increases by steps of $0.2\rho_0$ from left to right between 0.4 and $1.6\rho_0$. In each box the points correspond to temperature increases by steps of $0.10m_\pi$ between 0.05 and $1.05m_\pi$.

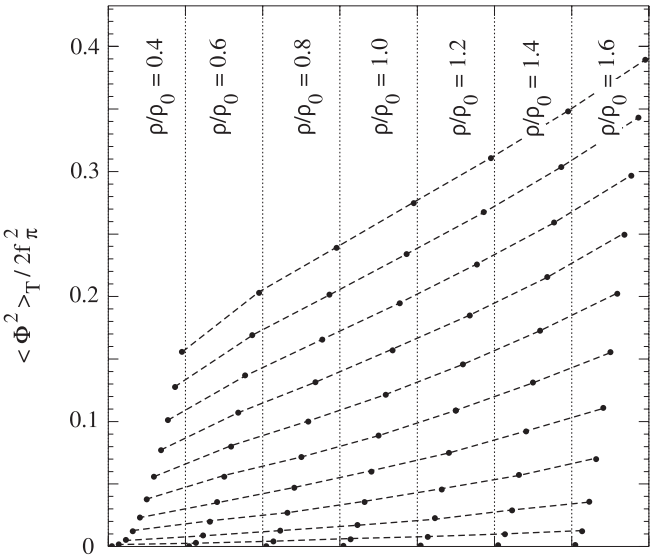

Fig. 9. Same as the preceding figure but for the thermal pions. As a guidance in order to display the influence of the density on the thermal pions, points of equal temperature are joined by a dashed line.

The iso-temperature curves show the influence of the baryonic density which pushes down the quasi-pion excitation energy, thus increasing their thermal excitation.

Finally in the last figure (fig. 10) we present the sum of both contributions. The competition between the variations of both terms with respect to the temperature is the source of the observed parabolic-type shape. For comparison, we have plotted in open circles the approximation of

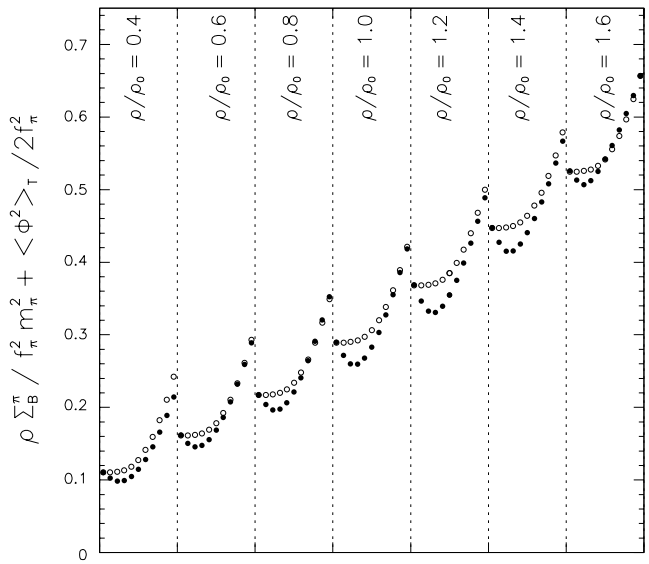

Fig. 10. Sum of both contributions of the virtual pion cloud and the thermal pions (black circles). For comparison the open circles represent the additive approximation of eq. (3)

eq. (3) where the effect of the thermal pions at zero density is simply added to that of the pion cloud at zero temperature. This approximation does not display the hollow shape of the exact calculation: it overestimates the latter by at most 15% in the medium part of the temperature range we have considered, the deviation becoming quite small beyond $T \approx 90$–$100\,\mathrm{MeV}$. In this region the decrease of the pionic cloud contribution with temperature (fig. 8) practically compensates the enhancement of the thermal excitations by density effects. The most important conclusion which can be drawn from fig. 10 is that, due to the nuclear pions, the pion scalar density is much larger than in the absence of nuclear effects, already for densities of the order of $0.6\rho_0$.

5 Conclusion

In conclusion we have studied the evolution of the quark condenaste of pionic origin under the simultaneous influence of the baryonic density and temperature. It is related to the scalar pionic density which comes on the one hand from the virtual nuclear pions and on the other hand from the thermally excited ones. We have expressed the first contribution in terms of the nuclear response to a pion-like excitation and evaluated it for the case of nuclear matter in the RPA scheme, first at zero and then at finite temperature. We have shown that the RPA produces a sizeable enhancement ($\approx 30\%$), while instead the temperature washes out the peaks and suppresses the nuclear response, hence decreasing the virtual pion density.

As for the thermally excited pions we have shown that the presence of the baryonic background appreciably enhances their number. The cause has to be found in the lowering of the quasi-pion excitation energies, which favours their thermal excitation. When the densities of both types

of pions are added, the mutual influences which go in opposite directions cancel their effects to a large extent. In the density and temperature domain that we have explored, the additive assumption of eq. (3) which neglects the mutual influence is a good approximation. It deviates from the exact result by no more than 15%, the deviation being maximum around $T \approx 50\,\mathrm{MeV}$. At this T value the additive approximation slightly overestimates the pionic density.

Our study has shown that, even at moderate baryonic density, the virtual nuclear pions are a major component of the overall scalar pion density. As an example, at nuclear matter density, they dominate in the temperature range we have considered, *i.e.* up to at least $T \approx 150\,\mathrm{MeV}$. Since the pion is the agent for the mixing of the vector and axial correlators, the consequence of our study is that the existence of a baryonic background, if any, should not be ignored in this mixing.

References

1. G. Chanfray, M. Ericson, Nucl. Phys. A **556**, 427 (1993).
2. G. Chanfray, M. Ericson, J. Wambach, Phys. Lett. B **388**, 673 (1996).
3. M. Dey, V.L. Eletsky, B.L. Ioffe, Phys. Lett. B **252**, 620 (1990).
4. G. Chanfray, J. Delorme, M. Ericson, Nucl. Phys. A **637**, 421 (1998).
5. G. Chanfray, D. Davesne, Nucl. Phys. A **646**, 125 (1999).
6. T. Ericson, W. Weise, *Pions and Nuclei* (Oxford Science Publications, Clarendon Press, Oxford, 1988).
7. M. Birse, J. Mc Govern, Phys. Lett. B **292**, 242 (1992).
8. I. Jameson, G. Chanfray, A.W. Thomas, J. Phys. G **18**, L159 (1992).
9. G. Chanfray, J. Delorme, M. Ericson, Phys. Lett. B **455**, 39 (1999).
10. J. Delorme, P.A.M. Guichon, Phys. Lett. B **264**, 157 (1991); more details and earlier references can be found in the unpublished report LYCEN 8906 (1989).
11. E. Oset, L.L. Salcedo, D. Strottman, Phys. Lett. B **165**, 13 (1985).
12. K. Shimizu, A. Faessler, Nucl. Phys. A **306**, 311 (1978); **333**, 495 (1980).
13. W.M. Alberico, M. Ericson, A. Molinari, Phys. Lett. B **92**, 153 (1980).
14. M. Ericson, in *Proceedings of the International School Mesons, Isobars, Quarks and Nuclear Excitations, Erice, 1983*, edited by D. Wilkinson (Pergamon Press 1983).
15. A.L. Fetter, J.D. Walecka, *Quantum Theory of Many-Particle Systems* (McGraw-Hill, New York 1971).